Journal of Applied Physics ARTICLE scitation.org/journal/jap

Impact of defects on the electrical properties of p–n diodes formed by implanting Mg and H ions into N-polar GaN

Cite as: J. Appl. Phys. **126**, 125102 (2019); doi: 10.1063/1.5116886
Submitted: 28 June 2019 · Accepted: 3 September 2019 ·
Published Online: 23 September 2019

Hiroko Iguchi (井口紘子),[1,a)] Tetsuo Narita (成田哲生),[1] Keita Kataoka (片岡恵太),[1] Masakazu Kanechika (兼近将一),[1] and Akira Uedono (上殿明良)[2]

AFFILIATIONS

[1]Toyota Central R&D Labs., Inc., Yokomichi, Nagakute 480-1192, Japan
[2]Division of Applied Physics, Faculty of Pure and Applied Science, University of Tsukuba, Tsukuba, Ibaraki 305-8573, Japan

[a)]**E-mail:** e4745@mosk.tytlabs.co.jp

ABSTRACT

The relationship between the junction properties and point defects in p–n diodes, formed by implanting magnesium (Mg) and hydrogen (H) ions into a GaN layer, was investigated. Vertical diodes were fabricated by implanting Mg ions with and without H ions into nitrogen-polar n-type GaN substrates, followed by annealing at 1150 °C or 1230 °C without the use of protective layers. Samples annealed at 1150 °C showed Schottky-barrier-diode (SBD)-like properties with an insufficient build-in potential, indicating surface depletion due to poor activation of Mg acceptors. The Mg/H-ion-implanted diode annealed at 1230 °C exhibited an improved rectifying property with a build-in potential around 3 V, close to an ideal p–n junction of GaN, whereas the sample with only implanted Mg-ions exhibited mixed properties of a p–n junction and SBD due to imperfect activation. In addition, leakage currents in the forward bias below 3 V for the Mg/H-ion-implanted diodes can be explained by a recombination current based on the Shockley–Read–Hall model with an estimated recombination lifetime of 3 to 10 ps. To clarify the sources of the difference in the junction properties, positron annihilation spectroscopy was employed. The samples annealed at 1150 °C contained high-density vacancy clusters such as $(V_{Ga}V_N)_3$, whose concentrations were reduced by the higher temperature annealing. We found that introduced H atoms can enhance the activation of Mg acceptors and/or reduce the defect concentrations. The results indicate the combination of the H ion introduction and higher temperature annealing improves the junction properties.

I. INTRODUCTION

Gallium nitride (GaN)-based metal–oxide–semiconductor field-effect transistors (MOSFETs) have attracted significant attention for use in high-power devices in next-generation electric systems including in-vehicle applications.[1] To approach the unipolar limit of GaN represented by Baliga's figure of merit,[2] selective-area doping techniques in power devices are required, which allows the fabrication of n-type or p-type regions, such as ohmic contacts, body regions to control the threshold voltage of MOSFETs,[3,4] current blocking layers,[5,6] and/or reduced surface field (RESURF)[7] structures in lateral MOSFETs. One process to achieve such structures is epitaxial regrowth techniques in selective areas, which have been demonstrated in several reported GaN power devices.[8–10] However, these techniques have some challenges in terms of the process cost and the controllability for fabricating MOSFETs. Ion implantation technology is a common process to locally form p–n junctions or contact regions in silicon- and SiC-based power devices.[11] In the case of ion implantation into GaN, especially the introduction of p-type dopants such as magnesium (Mg) ions, residual implantation damage after annealing could reduce the device performance and/or cause unstable operation due to the trapping of carriers into defect state levels under an applied voltage.[12,13] Therefore, reducing implantation-induced defects is crucial for realizing a GaN-based device with an ideal performance based on device simulations.

As a stage prior to applying ion implantation to device processes, a proper evaluation of implantation-induced damage for GaN is necessary to ensure good device performance. Rutherford backscattering spectrometry (RBS) is a common analytical method

to evaluate the crystallinity of implantation samples.[14,15] However, since GaN has an amorphous threshold two to three orders of magnitude higher than that of GaAs,[16] the ion channeling spectrum even for an as-implanted sample within the range of dosage used in device fabrication was only slightly different from that of an unimplanted sample.[17,18] The peak full-width of half maximums (FWHMs) of phonon modes in a Raman spectrum had also been used as indicators of recovery in crystal quality through annealing.[19] Recently, analytical methods sensitive to implantation-induced defects have been applied and have clarified the transformation of defect states through thermal annealing processes.[20–32] Through a photoluminescence (PL) examination, Kojima *et al.*[20] revealed that spectra for samples processed by Mg ion implantation with subsequent annealing commonly exhibit a green luminescence band related to nitrogen vacancies (V_Ns) and their complexes and a suppressed near-band-edge emission due to high-density nonradiative recombination centers (NRCs). Using cathodoluminescence (CL), Kataoka *et al.*[21] found that prolonged annealing at high temperature was effective for promoting the formation of Mg acceptors and suppressing the additional generation of V_N complexes. Chen *et al.*[22] revealed by cross-sectional CL observation that Mg acceptor related emission is observed at threading dislocations because Mg atoms diffuse along dislocations. Using PL measurement, Jacobs *et al.*[23] showed that activation of Mg ions was more readily achieved for N-polar films compared to for Ga-polar films. Sumiya *et al.*[24] detected the change of ion-implanted-induced defects through annealing within the bandgap of GaN using the photothermal deflection spectroscopy (PDS). Some researchers have investigated the defect levels formed through annealing after Mg ion implantation with a smaller dosage than the concentration of an n-type dopant.[25,26] Using positron annihilation spectroscopy (PAS) analysis, Uedono *et al.*[27,29] identified that divacancies, $V_{Ga}V_N$, are mainly formed in as-implanted GaN samples, and an agglomeration of vacancies occurs by annealing at more than 1273 K, leading to the formation of vacancy clusters such as $(V_{Ga}V_N)_3$. Shima *et al.*[30] suggested that such vacancy clusters have a large electron capture cross section of a few times 10^{-13} cm^2. Through transmission electron microscope (TEM) observations, Kumar *et al.*[31] found that Mg-rich pyramidal and line defects are formed in samples prepared by Mg ion implantation and subsequent annealing at 1623 K. Wang *et al.*[32] visualized the extended defects formed through postimplantation annealing using Fourier transform TEM images. These researches have clarified some of the common defects likely formed through Mg ion implantation and subsequent annealing.

The electrical characterization of p–n junctions formed by ion implantation is important for the application of actual devices. The junction properties have mainly been evaluated through the rectifying properties of Mg-ion-implanted p–n diodes.[13,33–36] Although some research has presented the rectification in the current–voltage (I–V) characteristics on the linear scale,[33–35] there have only been a few reported detailed analyses of I–V curves on a semilogarithmic scale.[13,36] Nakamura *et al.*[36] showed that junctions fabricated through Mg ion implantation and subsequent annealing at 1503 K consist of a homogeneous p-type area and small n-type areas, resulting in I–V curves that include components of p–n junctions and a parasitic Schottky barrier diode (SBD). Our research group[13] demonstrated that a p–n junction prepared by Mg and hydrogen (H) ion implantation had an ideality factor close to 2 in the range of 1.9 to 2.4 V due to the hole–electron recombination currents unique to the p–n junction, although the reason for the improved junction properties by introducing H ions is unclear. We also demonstrated the presence of high-density point defects near the p–n junction from the hysteresis of the capacitance–voltage (C–V) curve. However, the residual point defects near the junction are still not identified.

In most previous research, the analyses of implantation-induced defects and the electrical properties of p–n junctions have been separately discussed. To achieve high-quality p–n junctions to fulfill the specifications of devices, their relationship should be clarified, especially for understanding the H ion effect. In the present paper, we precisely discuss the relation between the electrical properties of Mg-ion-implanted junctions and the defect states by combining the electrical characterization and PAS analyses. We also discuss the impact of sequential H ion implantation on the electrical properties and its possible mechanisms.

II. EXPERIMENT

Samples were prepared by implanting Mg ions with and without H ions into N-polar n-type GaN(000−1) substrate through a 30-nm-thick SiN film deposited by plasma chemical vapor deposition (CVD) in order to avoid the decrease in Mg concentration at the surface. Figure 1 shows the depth profile of Mg and H atoms in an as-implanted sample and an annealed sample at 1230 °C after implantation of Mg/H atoms detected by secondary ion mass spectrometry (SIMS). The Mg ions were implanted with energies of 30 and 60 keV, with respective dosages of 3.5×10^{13} and 6.5×10^{13} cm^{-2}, to produce a maximum concentration of 1.4×10^{19} cm^{-3} at the near surface.[13] The implantation of H ions was performed after implanting Mg ions by introducing H_2 gas at 7 keV with a dosage of 7.0×10^{14} cm^{-2}, to yield a maximum concentration of 2.1×10^{20} cm^{-3}.[13] After the implantation, the SiN film was removed by dipping the samples in a buffered hydrogen fluoride solution. The Mg ions with and without H ion implantation samples were annealed at 1150 °C or 1230 °C for 30 s in N_2 gas under atmospheric pressure. No protective layer was required due to the high thermal stability of the N-polar surface.[37] There was no noticeable change in the Mg profile after annealing at 1230 °C as shown in Fig. 1(a). On the other hand, the H concentration shown in Fig. 1(b) decreased after high-temperature annealing except for the near-surface region involving the surface contamination. Hereinafter, the sample annealed at 1150 °C after Mg and H ion implantation is labeled as "1150 °C-Mg/H." Similarly, the other samples are indicated as "1150 °C-Mg," "1230 °C-Mg/H," and "1230 °C-Mg." Figure 2 shows a schematic of a fabricated diode with a vertical junction. Diodes were fabricated by depositing Ni/Au metal stacks as 200-μm-diameter circular anodes on the implanted surfaces, followed by the deposition of Ti/Al/Ni stacks as cathodes on the back of the substrates. Both electrodes were annealed to form ohmic contacts. Firstly, I–V measurements were performed at room temperature for these samples to investigate the effect of annealing temperature and H ion introduction. Especially, the component of the recombination current in the forward bias region was precisely compared with an epitaxial growth sample

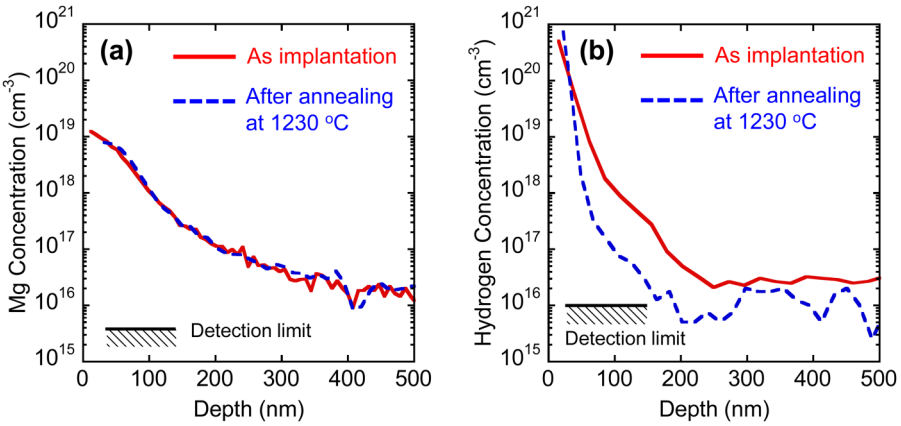

FIG. 1. Depth profiles of Mg and H atoms obtained from SIMS analysis for the samples before and after annealing.

reported previously.[38] Next, PAS analysis, which is a powerful technique for identifying vacancy-type defects, was performed on the 1150 °C-Mg/H and the 1230 °C-Mg/H samples to investigate the relationship between the junction properties and the implantation-induced point defects. Details on the PAS technique have been presented by Tuomisto and Makkonen[39] and Krause-Rehberg and Leipner[40] From the Doppler broadening spectra of the annihilation radiation, line-shape parameters (S) characterizing the defect concentrations were extracted as a function of the incident positron energy E, as well as the depth in darkness, where the S parameter was defined as the fraction of annihilation events over the energy range 510.24–511.76 keV. Positron annihilation coincidence Doppler broadening (CDB)[40] measurements were also performed at $E = 7$ keV, corresponding to 120 nm of mean depth, with and without illumination with a 325-nm He–Cd laser with an irradiance of 10 mW/cm^2. The CDB analysis gave precise S and wing (W) parameters, allowing the assignment of the defect types by reference to a calculated database of vacancies reported previously, where the W parameter was defined as the fraction in the range 513.28–515.56 keV.[29,41]

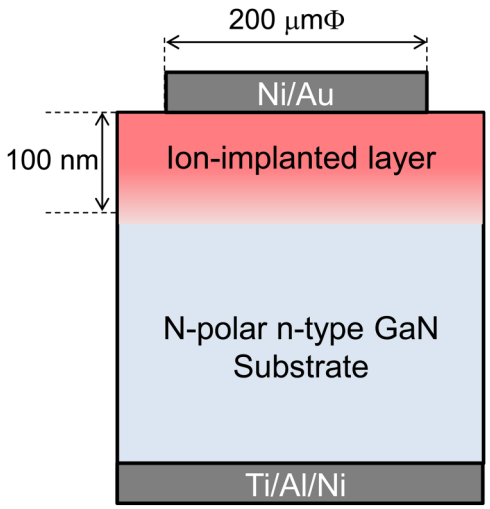

FIG. 2. Schematic of the fabricated diode.

III. RESULTS AND DISCUSSIONS

The I–V curves for each sample were plotted on both linear and semilogarithmic scales, as shown in Fig. 3. The 1150 °C-Mg and 1150 °C-Mg/H diodes exhibited turn-on voltages of less than 1 V, like an n-type SBD as plotted on a linear scale in Fig. 3(c), while there were slight differences in the leakage currents on the semilogarithmic scale as shown in Fig. 3(a). Namely, the leakage current for the 1150 °C-Mg/H diode for reverse bias and forward bias below the turn-on voltage was much lower than that for the 1150 °C-Mg diode. In other words, the 1150 °C-Mg/H diode had a higher build-in potential, which was slightly different from that of a simple n-type SBD. On the other hand, the turn-on voltages of the 1230 °C-Mg and 1230 °C-Mg/H samples were much higher than those of samples annealed at 1150 °C on the linear scale, as shown in Fig. 3(d). In the samples annealed at 1230 °C, the H-implanted samples showed a much lower leakage current than the Mg-implanted diode on the semilog scale in Fig. 3(b) and exhibited a turn-on voltage of around 3.2 V, close to the ideal build-in potential of a GaN p–n junction, as shown in Fig. 3(d). These results suggest two facts: (i) there is a threshold annealing temperature to activate Mg acceptors in GaN between 1150 °C and 1230 °C. (ii) Hydrogen introduction reduces the leakage current. This threshold temperature is consistent with the fact that the annealing was performed over 1200 °C in the previous reports indicating p-type formation.[35,36,42–46] We believe that the Mg acceptor concentrations can exceed the concentration of donorlike point defects above this threshold annealing temperature, which possibly depends on the implantation conditions, such as the dosage. From this point of view, the combination of Mg and sequential H ion implantation can lead to the effective activation of Mg acceptors and/or reducing the number of donorlike point defects compensating holes near the p–n junction. This change was observed even in the 1150 °C-Mg/H diode having imperfect junction properties.

To understand the obtained I–V characteristics, we made a simple estimation of the average effective acceptor concentration

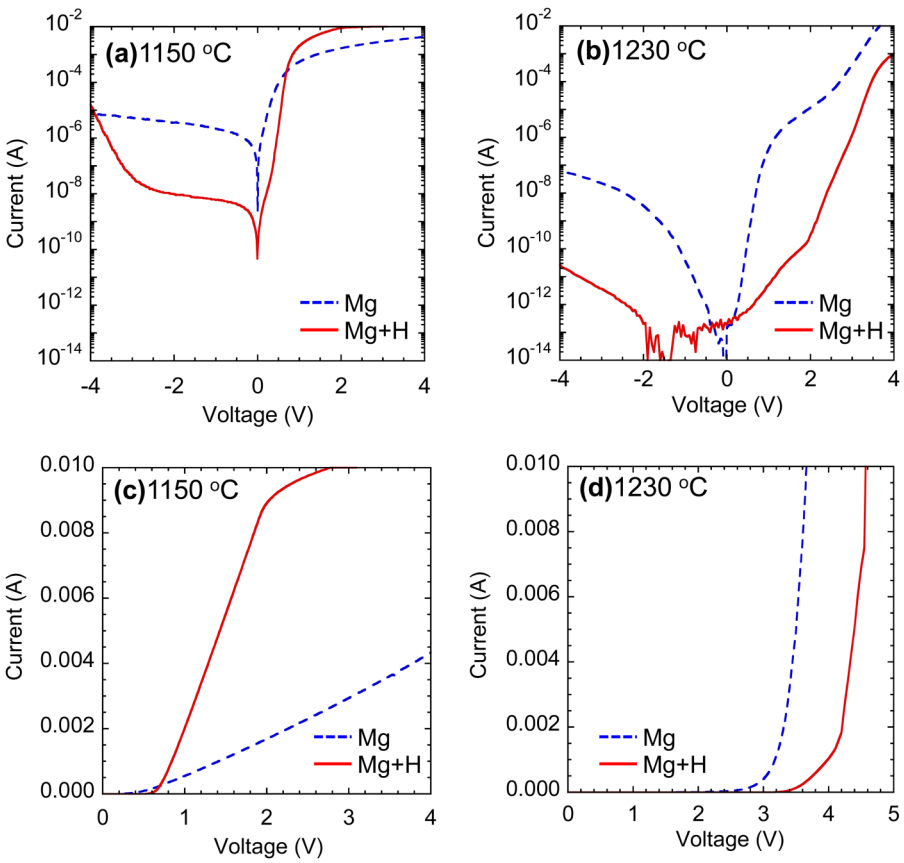

FIG. 3. *I–V* characteristics on (a), (b) semilogarithmic scale, and (c) and (d) linear scale for each sample produced using annealing at 1150 °C after Mg or Mg/H implantation into a GaN(000−1) substrate [(a) and (c)] and annealing at 1230 °C after Mg or Mg/H implantation into a GaN(000−1) substrate [(b) and (d)].

$(N_A - N_D)$ for each diode, where N_A and N_D are the acceptor and net donor concentrations, respectively. Into the substrate with a donor impurity concentration of 9.7×10^{16} cm^{-3}, the implantation layer is completely depleted at 0 V when average $N_A - N_D$ is less than 1.5×10^{17} cm^{-3} in the 100 nm of near-surface region. Note that $N_A - N_D$ can be determined from the difference between the Mg acceptor concentration and the total concentration (N_D) of donor impurities and donorlike defects induced through the ion implantation and the subsequent annealing. The barrier height (Φ_B) of 1150 °C-Mg and 1150 °C-Mg/H estimated from the I-V characteristics in Fig. 3(a) were 0.58 and 0.84 eV, respectively. The higher Φ_B in the 1150 °C-Mg/H sample was possibly caused by partial activation of Mg ions as acceptors. However, the Φ_B value of the 1150 °C-Mg/H sample is much lower than the turn-on voltage of a GaN-based p-n diode. Thus, $N_A - N_D$ for the 1150 °C-Mg/H sample might be below 1.5×10^{17} cm^{-3}. Such imperfect activation leads to the formation of a junction with a built-in potential between that of a p–n diode and an SBD, as shown in Fig. 4(a). On the other hand, the turn-on voltage of around 3.2 V on the linear scale for the 1230 °C-Mg/H sample indicates the formation of a p–n junction close to an ideal state, as shown in Fig. 4(b), indicating a value of $N_A - N_D$ above 1.5×10^{17} cm^{-3} for the whole device area. In contrast, the turn-on voltage for the 1230 °C-Mg sample was slightly lower than 3 V, and the current for the forward voltage increased in two steps, as shown in Fig. 3(b). This indicates that the 1230 °C-Mg diode was composed of a p–n junction and some imperfect areas having $N_A - N_D$ less than 1.5×10^{17} cm^{-3}. Nakamura *et al.*[36] mentioned that such *I–V* characteristic can be expressed as a parallel circuit having a p–n diode and an SBD with series resistances. These results suggest that H introduction can promote activation of Mg ions as acceptors and/or reduce the compensation donor concentrations due to the ion-implantation-induced defects.

A detailed *I–V* analysis for the 1230 °C-Mg/H sample was carried out in order to compare it with a p–n diode formed by epitaxial growth reported previously.[38,47] For a p–n diode fabricated by epitaxial growth, a recombination current at the p–n junction originates from the recombination of electron–hole pairs based on the Shockley–Read–Hall (SRH) model. That is, the SRH lifetime is determined by both the concentration of recombination centers and the capture cross section. Hu *et al.*[47] reported that an SRH lifetime of 12 ns in homoepitaxial n-type GaN at room temperature can be extracted from the *I–V* characteristic of a p+/n− junction diode fabricated by a metalorganic vapor phase epitaxy (MOVPE) method. Maeda *et al.*[38] also estimated the SRH lifetime for homoepitaxial p-type GaN to be 46 ps at 298 K from the *I–V* properties of a p/n+ junction diode formed by MOVPE. The large difference in lifetimes for both conductive layers is mainly due to the difference

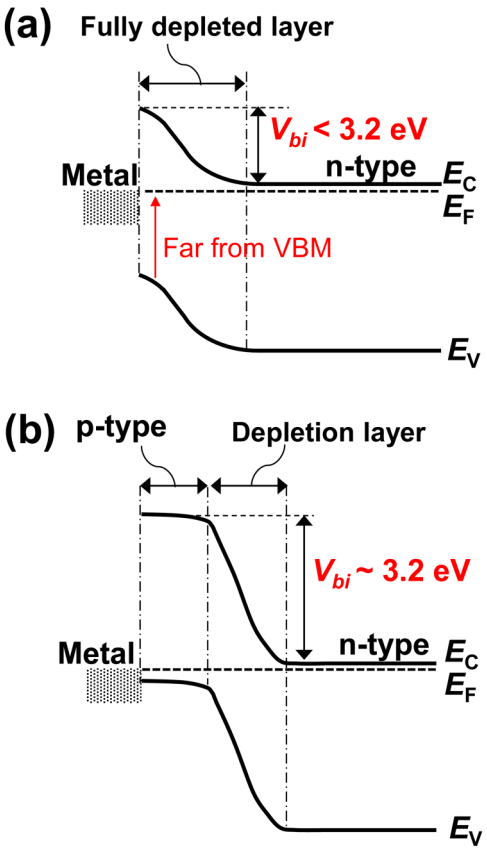

FIG. 4. Band diagrams of Mg-ion-implanted p-n diodes for (a) a fully depleted state in the implanted layer and (b) an ideal PN junction state. The implanted layer is fully depleted when the average $N_A - N_D$ value is lower than 1.5×10^{17} cm^{-3}, which is the upper limit concentration of full depletion in the implanted layer in the present study. In the case of (a), Fermi level (E_F) is far from the valence band maximum (VBM) even near the surface, and the built-in potential (V_{bi}) is likely to be lower than the ideal value of around 3.2 eV. On the other hand, the V_{bi} in the ideal PN junction is nearly 3.2 eV, as shown in (b), so that the turn-on voltage of the p-n diode becomes higher than that in (a).

in capture cross sections of SRH recombination centers for holes and electrons.[38,48] Their analytical works can become good references for the present study because the MOVPE–grown p–n junction on a GaN substrate has much ideal property compared to the ion implanted samples. In the present paper, the SRH lifetime in the 1230 °C-Mg/H sample was extracted from the I–V characteristic using the analytical method reported by Hu *et al.*[47] and Maeda *et al.*[38] The recombination current density of a p–n diode is mainly dominated by J_{SRH}, which represent the SRH recombination current density. J_{SRH} can be written as[38]

$$J_{SRH} \sim \frac{\pi n_i kT}{2\tau_{SRH} F_0} \exp\left(\frac{qV}{2kT}\right), \tag{1}$$

where $\tau_{SRH} = \sqrt{\tau_p \tau_n}$ is used. τ_p and τ_n are the lifetimes of holes and electrons, respectively. The factor of 2 in the denominator represents an ideality factor due to the recombination current. n_i is the intrinsic carrier concentration in GaN, and q and k are the electric charge and the Boltzmann constant, respectively. V is the applied voltage and F_0 is the electric field at the position where electron–hole pairs most likely recombine. To extract τ_{SRH}, Maeda *et al.*[38] calculated F_0 at the recombination position based on a one-sided abrupt junction formed by an MOVPE method. In the present case, the concentric profile of acceptors formed by the implantation techniques was gradually decreased in the depth direction, resulting in a gradual change in the electric field. Since it is difficult to determine the accurate concentric profile, we assumed a linearly graded junction to calculate the electric field in the 1230 °C-Mg/H sample. The depletion layer width (W) as a function of forward bias was calculated from the C–V curve as shown in Fig. 5. The relationship between the applied voltage (V_a) and the maximum of the electric field (F_{max}) was represented as

$$V_a = \frac{2}{3} W F_{max}. \tag{2}$$

In the present study, we assumed $F_0 = F_{max}$ in Eq. (1).

Figure 5 shows three J–V curves obtained from different positions in the same sample of 1230 °C-Mg/H. The dashed line in Fig. 5 shows the components of the recombination current calculated for τ_{SRH} = 1–20 ps based on Eq. (1). In the range of 2–2.4 V, the slopes of the J–V curves were close to the calculations, indicating the existence of the recombination current. τ_{SRH} in the 1230 °C-Mg/H sample was estimated to be 3–10 ps. The obtained value might be slightly underestimated due to the leakage current and can involve an error of about half to the few times due to the inaccuracy of F_0 estimation. Since the implanted p-type layer is likely more defective compared with the underlying n-type layer, the

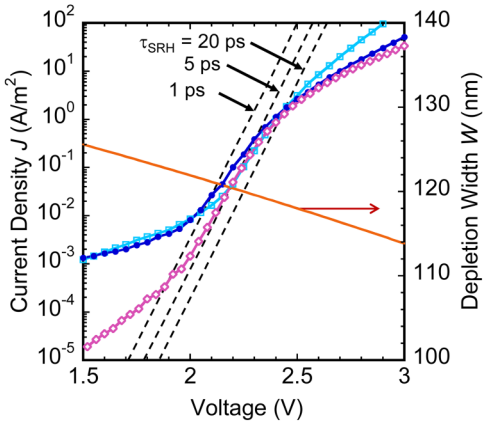

FIG. 5. Forward J–V characteristics (lines with symbols) in the p-n diode fabricated by annealing at 1230 °C after implantation of Mg/H ions. Three different datasets were obtained from different positions in the same sample. The solid line without symbols shows the voltage dependence of the depletion width W obtained from a C–V curve.[13] The dashed lines having a slope of the ideality factor of 2 indicate the calculated recombination currents for τ_{SRH} = 1, 5, and 20 ps based on the SRH recombination model.

recombination plausibly occurs in the p-type side. The obtained τ_{SRH} value (3–10 ps) is much shorter than the reported value in MOVPE grown p-type GaN (46 ps)[38] even with consideration of inaccuracy in the estimation. Therefore, the shorter lifetime compared with the epitaxial sample was mainly due to the high-density SRH recombination centers formed by ion-implantation and postannealing, even in the 1230 °C-Mg/H sample. In addition, the 1230 °C-Mg/H sample had a much narrower voltage range for which $\eta = 2$ compared with the MOVPE-grown p–n diode in which $\eta = 2$ in the range 1.8–2.7 V, as reported by Maeda *et al.*[38] This resulted from the considerable leakage current for the 1230 °C-Mg/H sample, which might be caused by the implantation-induced defects.

In order to identify the point defects generating the difference in the electrical properties, PAS analyses were performed. Figure 6 shows the *S* values as a function of incident positron energy *E* for the 1150 °C-Mg/H and 1230 °C-Mg/H samples. The mean implantation depth of positrons is also shown by the upper horizontal axis in Fig. 6. The previous research showed that the *S* value in high-quality GaN grown by hydride vapor phase epitaxy (HVPE) on a GaN seed wafer has an *S* value of 0.442.[49] On the other hand, an *S* value much higher than 0.442 suggests positron trapping by vacancy-type defects introduced by the ion-implantation and postannealing.[29,41] In the as-implanted state, the *S* values were much higher than in the defect-free state, indicating the introduction of high-density vacancies, where the mean depth having higher *S* values was estimated to be 850 nm from the previous simulation of *S*–*E* curve.[41] Although the *S* values after annealing as well as the defect densities were reduced, there was a significant difference between samples annealed at different temperatures. The *S* value of the 1150 °C-Mg/H sample was larger than that of the 1230 °C-Mg/H sample, especially in the range of *E* from 0 to 7 keV, as shown in Fig. 6. Uedono *et al.*[27] reported that the defect charged states in a Mg-ion-implanted layer tend to be positive if the Fermi level approaches the valence band maximum (VBM). Since positrons are not likely captured by the positively charged defects, the *S* value is decreased. Therefore, the lower *S* value of the 1230 °C-Mg/H sample at around $E = 2$ keV can be attributed to both the enhanced activation of Mg acceptors and the decreased defect density. Since such a local minimum of *S* parameters in the near surface region was not clearly observed for the 1150 °C-Mg/H sample, the Fermi level was probably far from the VBM due to insufficient activation of the Mg acceptors. These results can reasonably explain the improved rectifying property of the 1230 °C-Mg/H sample and the insufficient turn-on voltage of the 1150 °C-Mg/H sample. On the other hand, the increase of the *S* parameter near the junctions (E~7 keV) for both the annealed samples indicates that the defect density was higher near the junction.

Figure 7 shows the *S*–*W* relationships for as-implanted diode and the 1150 °C-Mg/H and 1230 °C-Mg/H samples in darkness and under illumination of $E = 7$ keV. The result for HVPE GaN is also shown as "DF." The calculated (*S*,*W*) values for the annihilation of positrons in the delocalized state "*DF*(cal.)," typical cation vacancies, such as V_{Ga} and $(V_{Ga})_m(V_N)_n$ (m, n: integer), and hydrogenated vacancy-type defects are also shown in Fig. 7 (blue symbols), the same as the previous report.[41] The difference between "*DF*" and "*DF*(cal.)" could be due to several causes, such as the limitations of the simulation and the background noise of the Ge detectors.[29,41] As Uedono *et al.*[27,29] reported previously, the major defect in the as-implanted sample was V_{Ga}-related defects such as

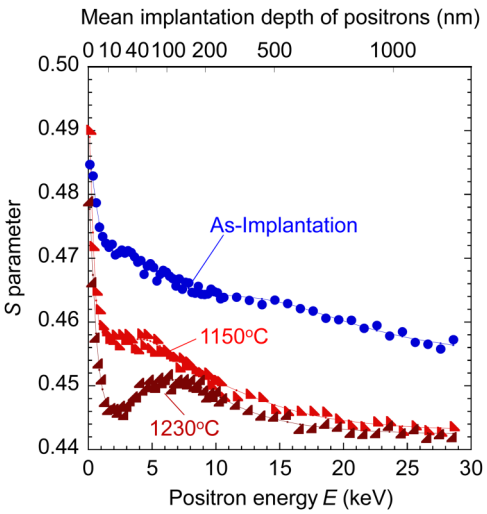

FIG. 6. *S* parameters as functions of incident positron energy *E* and mean implantation depth of positrons for the as-implanted sample (closed circles) and annealed samples (triangles) at 1150 °C and 1230 °C after implanting Mg and H ions. In the 1230 °C-Mg/H sample, the local minimum value around $E = 2$ keV indicates a decrease of positron trapping due to the formation of a p-type region as well as a lowering of the Fermi level near the surface, as shown in Fig. 4(b).

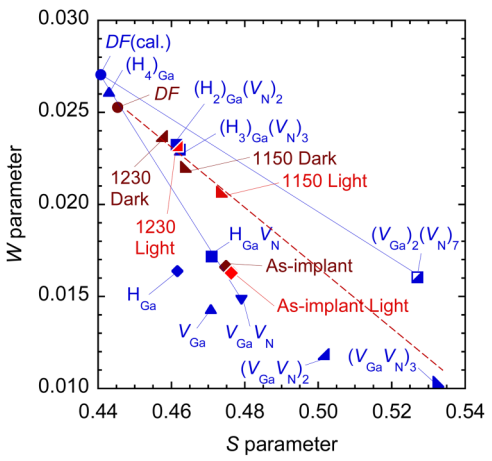

FIG. 7. (*S*,*W*) values for as-implanted sample ("As-implant") and samples annealed at 1150 °C and 1230 °C after implantation of Mg and H ions (brown and red triangles) in darkness (Dark) and under illumination (Light). The closed blue symbols are the calculated (*S*,*W*) values as reported in Ref. 41. The label "*DF*" for a brown circle indicates the (*S*,*W*) value obtained from HVPE-grown freestanding GaN.[41] The dashed line is a guideline connecting the (*S*,*W*) values for the annealed samples and the "*DF*."

divacancies ($V_{Ga}V_N$). Actually, the (S,W) value of the as-implanted sample was located near the line between DF(cal.) and $V_{Ga}V_N$. On the other hand, the large vacancy clusters of average size $(V_{Ga}V_N)_3$ with a size of 0.79 nm were on the extension of the line connected with the (S,W) values of the DF and the annealed samples. Note that there exists various sizes of vacancy clusters and the PAS can only give their average size. Since the (S,W) value is a characteristic value for those states,[39,40] the major defect in both annealed samples was such vacancy clusters, corresponding to the previous reports.[29] However, the positively charged defects as well as the donorlike defects in an Mg-ion implanted layer likely lead to underestimation of the defect concentration. Illumination by a light source with a photon energy above the bandgap is effective for detecting such hidden defects because the illumination causes transitions in the charge states of vacancy-type defects from positive to neutral (or neutral to negative), i.e., $V^+ \rightarrow V^0$ (or $V^0 \rightarrow V^-$).[29,41] The S values of the 1150 °C-Mg/H and 1230 °C-Mg/H samples shifted to positive under illumination on the same line connecting DF and $(V_{Ga}V_N)_3$, indicating the successful detection of the hidden donorlike defects in the dark. We already mentioned that a p-n diode with sufficient build-in potential requires the average $N_A - N_D$ value above 1.5×10^{17} cm^{-3}. Based on the weighted average of DF and $(V_{Ga}V_N)_3$,[30,39] the defect concentration for the 1150 °C-Mg/H sample was a few times higher than that for the 1230 °C-Mg/H sample. If there is a donorlike defect concentration close to this concentration, these defects can act as a significant compensation source, resulting in insufficient build-in potential for the 1150 °C-Mg/H sample as illustrated in Fig. 4(a). If the concentration of vacancy clusters such as $(V_{Ga}V_N)_3$ is sufficiently lower than the $N_A - N_D$ value needed to get an ideal build-in potential for a p–n junction, we can obtain the rectification property with a turn-on voltage corresponding to the ideal build-in potential, which probably corresponds to the situation for the 1230 °C-Mg/H sample having good rectification, as shown in Fig. 3(b) and (d). Based on the I–V characteristics, the average compensating defect concentrations for the 1150 °C-Mg/H and 1230 °C-Mg/H are estimated to be likely to be close to 1.5×10^{17} cm^{-3} and 10^{17} cm^{-3} or less, respectively. Based on the order of compensating defect concentrations predicted from the illuminated (S,W) values for both samples, these estimates are acceptable. Uedono *et al.* also pointed out that the H-introduction leads to hydrogenation of the Mg and some of the vacancies such as $(H_2)_{Ga}(V_N)_2$ and $(H_3)_{Ga}(V_N)_3$ located near the line connecting DF and $(V_{Ga}V_N)_3$. Because the H concentrations after annealing at 1150 °C and 1230 °C were both below 10^{17} cm^{-3}, from SIMS analysis, the concentrations of hydrogenated vacancies accommodating two or three H atoms were at most a few times 10^{16} cm^{-3} for both Mg/H-implanted samples. Therefore, it is a reasonable conclusion that the major defects for the 1150 °C-Mg/H sample are $(V_{Ga}V_N)_3$, even based on the existence of hydrogenated vacancies. The 1230 °C-Mg/H sample might have a comparable concentration of hydrogenated vacancies. In this case, we obtain an improved rectification property compared to the 1230 °C-Mg sample, as indicated in Fig. 3(b). Accordingly, the hydrogenated vacancies do not negatively impact the junction properties.

Through PAS analysis, Uedono *et al.*[41] examined interactions between Mg, H, and vacancies by comparing Mg/H- and Mg-ion-implanted samples having 0.7-μm-deep box-shaped profiles. Then, the suppression of cluster formations such as $(V_{Ga}V_N)_3$ were clearly observed using H-introduction.[41] Based on this, we suggest that there are two major effects of H-introduction. The first is that the formation energy of Mg-substituted Ga sites (Mg_{Ga}) decreases by hydrogenation,[50] resulting in enhanced activation of Mg acceptors. The second is an increase of the formation energy for vacancies by hydrogenation of Mg_{Ga}. When Mg–H complexes are formed, the Fermi level is likely pinned near the midgap,[50] resulting in an increase in the formation energy of both donorlike and acceptorlike defects.[51] As a result, the agglomeration of vacancies is possibly suppressed during annealing compared to the case without H introduction. Both effects provide a reasonable explanation for the improved rectification in the Mg/H-implanted p-n diodes in the present paper. The H introduction thus increases the $N_A - N_D$ value by increasing the activation ratio of Mg acceptors and/or decreasing donorlike defects. However, remaining defects such as $(V_{Ga}V_N)_3$ and $(H_n)_{Ga}(V_N)_n$ might act as recombination centers based on the SRH model, resulting in a shorter lifetime for the 1230 °C-Mg/H sample compared with that for the MOVPE-grown p-n diode, as shown in Fig. 5. Accordingly, further developments in the process are required by optimizing the profile of H ions and increasing the annealing temperature.

IV. CONCLUSION

We investigated the relationship between the electrical junction properties in Mg- and H-ion-implanted samples and point defects induced through the implantation and the postannealing processes. Diodes with vertical junctions were fabricated by annealing at 1150 °C and 1230 °C after implanting Mg and Mg/H ions into N-polar n-type GaN substrates. The leakage currents at the applied voltage below the on-voltage were effectively suppressed by introducing H ions. Moreover, the turn-on voltage close to the ideal built-in potential of a GaN p–n junction was obtained by annealing with sample processing by implanting Mg/H-ions and subsequent annealing at 1230 °C, whereas the other samples exhibited insufficient build-in potentials. These differences could be explained by considering the band diagrams with different activation ratios of Mg acceptors. The best p-n diode was the 1230 °C-Mg/H sample, which exhibited a component of SRH recombination current having an ideality factor around 2. The SRH lifetime of this p-n diode was estimated to be 3–10 ps, which is shorter than that in the epitaxial p-type GaN layer reported previously, indicating that there were some residual recombination centers.

From the I–V characteristics, we estimated that the average compensating defect concentrations for 1150 °C-Mg/H and 1230 °C-Mg/H are likely close to 1.5×10^{17} cm^{-3} and 10^{17} cm^{-3} or less, respectively. Based on the order of compensating defect concentrations predicted from the illuminated (S,W) values for both samples from the PAS analysis, the estimations of the compensating defect concentrations are acceptable. Since the H-introduced diodes exhibited superior rectification properties than the diodes implanted only with Mg ions, the introduced H can passivate Mg atoms during annealing, likely resulting in the enhancement of the formation of Mg_{Ga} and/or reducing generation of donorlike vacancy clusters. This schematic gives a good explanation of the improved electrical properties of H-introduced p-n diodes. All the

results strongly suggest that the combination of H introduction and high-temperature annealing leads to an effective enhancing activation ratio of acceptors in the p–n junction formed by ion implantation.

ACKNOWLEDGMENTS

The authors would like to thank S. Ishibashi of the National Institute of Advanced Industrial Science and Technology (AIST) for providing the calculated data reported previously. This work was supported by the Council for Science, Technology and Innovation (CSTI), Cross-Ministerial Strategic Innovation Promotion (SIP) Program for "Next-Generation Power Electronics," funded by NEDO.

REFERENCES

[1]T. Kachi, Jpn. J. Appl. Phys. **53**, 100210 (2014).
[2]A. M. Ozbek and B. J. Baliga, IEEE Electron Device Lett. **32**, 300 (2011).
[3]M. Kanechika, M. Sugimoto, N. Soejima, H. Ueda, O. Ishiguro, M. Kodama, E. Hayashi, K. Itoh, T. Uesugi, and T. Kachi, Jpn. J. Appl. Phys. **46**, L503 (2007).
[4]M. Kodama, M. Sugimoto, E. Hayashi, N. Soejima, O. Ishiguro, M. Kanechika, K. Itoh, H. Ueda, T. Uesugi, and T. Kachi, Appl. Phys. Express **1**, 021104 (2008).
[5]S. Mandal, A. Agarwal, E. Ahmadi, K. M. Bhat, D. Ji, M. A. Laurent, S. Keller, and S. Chowdhury, IEEE Electron Device Lett. **38**, 933 (2017).
[6]M. H. Wong, K. Goto, H. Murakami, Y. Kumagai, and M. Higashiwaki, IEEE Electron Device Lett. **40**, 431 (2019).
[7]M. Noborio, J. Suda, and T. Kimoto, Appl. Phys. Express **1**, 101403 (2008).
[8]M. Okada, Y. Saitoh, M. Yokoyama, K. Nakata, S. Yaegasi, K. Katayama, M. Ueno, M. Kiyama, T. Katsuyama, and T. Nakamura, Appl. Phys. Express **3**, 054201 (2010).
[9]D. Ji, C. Gupta, S. H. Chan, A. Agarwal, W. Li, S. Keller, U. K. Mishra, and S. Chowdhury, IEEE Electron Device Lett. **37**(12), 1601 (2016).
[10]D. Shibata, R. Kajitani, M. Ogawa, K. Tanaka, S. Tamura, T. Hatsuda, M. Ishida, and T. Ueda, *IEDM Technical Digest* (IEEE, 2016), pp. 248.
[11]T. Kimoto, Jpn. J. Appl. Phys. **54**, 040103 (2015).
[12]M. Meneghini, A. Tajalli, P. Moens, A. Banerjee, E. Zanoni, and G. Meneghesso, Mater. Sci. Semicond. Process. **78**, 118 (2018).
[13]T. Narita, T. Kachi, K. Kataoka, and T. Uesugi, Appl. Phys. Express **10**, 016501 (2017).
[14]K. Pagowska, R. Ratajczak, A. Stonert, A. Turos, L. Nowicki, N. Sathish, P. Jozwik, and A. Muecklich, Acta Phys. Pol. A **120**, 153 (2011).
[15]N. Nishikata, K. Kushida, T. Nishimura, T. Mishima, K. Kuriyama, and T. Nakamura, Nucl. Instrum. Methods Phys. Res. Sect. B **409**, 302 (2017).
[16]C. Ronning, E. P. Carlson, and R. F. Davis, Phys. Rep. **351**, 349 (2001).
[17]H. H. Tan, J. S. Williams, J. Zou, D. J. H. Cockayne, S. J. Pearton, and R. A. Stall, Appl. Phys. Lett. **69**, 2364 (1996).
[18]J. C. Zolper, M. H. Crawford, J. S. Williams, H. H. Tan, and R. A. Stall, Nucl. Instrum. Methods Phys. Res. B **127/128**, 467 (1997).
[19]J. D. Greenlee, B. N. Feigelson, T. J. Anderson, M. J. Tadjer, J. K. Hite, M. A. Mastro, C. R. Eddy, Jr., K. D. Hobart, and F. J. Kub, J. Appl. Phys. **116**, 063502 (2014).
[20]K. Kojima, S. Takashima, M. Edo, K. Ueno, M. Shimizu, T. Takahashi, S. Ishibashi, A. Uedono, and S. F. Chichibu, Appl. Phys. Express **10**, 061002 (2017).
[21]K. Kataoka, T. Narita, H. Iguchi, T. Uesugi, and T. Kachi, Phys. Status Solidi B **255**, 1700379 (2018).
[22]J. Chen, W. Yi, T. Kimura, S. Takashima, M. Edo, and T. Sekiguchi, Appl. Phys. Express **12**, 051010 (2019).
[23]A. G. Jacobs, B. N. Feigelson, J. K. Hite, C. A. Gorsak, L. E. Luna, T. J. Anderson, and F. J. Kub, Jpn. J. Appl. Phys. **58**, SCCD07 (2019).
[24]M. Sumiya, K. Fukuda, H. Iwai, T. Yamaguchi, T. Onuma, and T. Honda, AIP Adv. **8**, 115225 (2018).
[25]G. Alfieri, V. K. Sundaramoorthy, and R. Micheletto, J. Appl. Phys. **123**, 205303 (2018).
[26]M. Akazawa, N. Yokota, and K. Uetake, AIP Adv. **8**, 025310 (2018).
[27]A. Uedono, S. Takashima, M. Edo, K. Ueno, H. Matsuyama, H. Kudo, H. Naramoto, and S. Ishibashi, Phys. Status Solidi B **252**, 2794 (2015).
[28]S. R. Aid, T. Uneme, N. Wakabayashi, K. Yamazaki, A. Uedono, and S. Matsumoto, Phys. Status Solidi A **214**, 1700225 (2017).
[29]A. Uedono, S. Takashima, M. Edo, K. Ueno, H. Matsuyama, W. Egger, T. Koschine, C. Hugenschmidt, M. Dickmann, K. Kojima, S. F. Chichibu, and S. Ishibashi, Phys. Status Solidi B **255**, 1700521 (2018).
[30]K. Shima, H. Iguchi, T. Narita, K. Kataoka, K. Kojima, A. Uedono, and S. F. Chichibu, Appl. Phys. Lett. **113**, 191901 (2018).
[31]A. Kumar, K. Mitsuishi, T. Hara, K. Kimoto, Y. Irokawa, T. Nabatame, S. Takashima, K. Ueno, M. Edo, and Y. Koide, Nanoscale Res. Lett. **13**, 403 (2018).
[32]Y. Wang, T. Bai, C. Li, M. J. Tadjer, T. J. Anderson, J. K. Hite, M. A. Mastro, C. R. Eddy, Jr., K. D. Hobart, B. N. Feigelson, and M. S. Goorsky, ECS J. Solid State Sci. Technol. **8**, 70 (2019).
[33]E. V. Kalinina, V. A. Solov'ev, A. S. Zubrilov, and V. A. Dmitriev, MRS Internet J. Nitride Semicond. Res. **4**(51), 751 (1999).
[34]T. Oikawa, Y. Saijo, S. Kato, T. Mishima, and T. Nakamura, Nucl. Instrum. Methods Phys. Res. B **265**, 168 (2015).
[35]J. D. Greenlee, B. N. Feigelson, T. J. Anderson, J. K. Hite, K. D. Hobart, and F. J. Kub, ECS J. Solid State Sci. Technol. **4**, 382 (2015).
[36]T. Nakamura, M. Yoshino, H. Tsuge, K. Ikeda, and K. Kuriyama, Surf. Coatings Technol. **355**, 7 (2018).
[37]H. Suzuki, R. Togashi, H. Murakami, Y. Kumagai, and A. Koukitu, J. Cryst. Growth **310**, 1632 (2008).
[38]T. Maeda, T. Narita, H. Ueda, M. Kanechika, T. Uesugi, T. Kachi, T. Kimoto, M. Horita, and J. Suda, Jpn. J. Appl. Phys. **58**, SCCB14 (2019).
[39]F. Tuomisto and I. Makkonen, Rev. Mod. Phys. **85**, 1583 (2013).
[40]R. Krause-Rehberg and H. S. Leipner, *Positron Annihilation in Semiconductors, Solid-State Sciences* (Springer-Verlag, Berlin, 1999), Vol. **127**.
[41]A. Uedono, H. Iguchi, T. Narita, K. Kataoka, W. Egger, T. Koschine, C. Hugenschmidt, M. Dickmann, K. Shima, K. Kojima, S. F. Chichibu, and S. Ishibashi, Phys. Status Solidi B 1900104 (2019).
[42]B. Skromme and G. L. Martinez, Optical activation behavior of ion implanted acceptor species in GaN, in *The 1999 MRS Fall Meeting, Boston, MA, USA* (Mater. Res. Soc. Symp. Proc., 1999), Vol. 595.
[43]M. J. Tadjer, B. N. Feigelson, J. D. Greenlee, J. A. Freitas, Jr., T. J. Anderson, J. K. Hite, L. Ruppalt, C. R. Eddy Jr., K. D. Hobart, and F. J. Kub, ECS J. Solid State Sci. Technol. **5**, 124 (2016).
[44]T. Niwa, T. Fujii, and T. Oka, Appl. Phys. Express **10**, 091002 (2017).
[45]M. Yoshino, Y. Ando, M. Deki, T. Toyabe, K. Kuriyama, Y. Honda, T. Nishimura, H. Amano, T. Kachi, and T. Nakamura, Materials **12**, 689 (2019).
[46]R. Tanaka, S. Takashima, K. Ueno, H. Matsuyama, M. Edo, and K. Nakagawa, Appl. Phys. Express **12**, 054001 (2019).
[47]Z. Hu, K. Nomoto, B. Song, M. Zhu, M. Qi, M. Pan, X. Gao, V. Protasenko, D. Jena, and H. G. Xing, Appl. Phys. Lett. **107**, 243501 (2015).
[48]S. F. Chichibu, K. Shima, K. Kojima, S. Takashima, M. Edo, K. Ueno, S. Ishibashi, and A. Uedono, Appl. Phys. Lett. **112**, 211901 (2018).
[49]K. Kojima, Y. Tsukada, E. Furukawa, M. Saito, Y. Mikawa, S. Kubo, H. Ikeda, K. Fujito, A. Uedono, and S. F. Chichibu, Appl. Phys. Express **8**, 095501 (2015).
[50]J. L. Lyons, A. Janotti, and C. G. Van de Walle, Phys. Rev. Lett. **108**, 156403 (2012).
[51]P. Reddy, M. P. Hoffmann, F. Kaess, Z. Bryan, I. Bryan, M. Bobea, A. Klump, J. Tweedie, R. Kirste, S. Mita, M. Gerhold, R. Collazo, and Z. Sitar, J. Appl. Phys. **120**, 185704 (2016).